BIOLOGY OF REPRODUCTION (2015) **93**(5):110, 1–10
Published online before print 23 September 2015.
DOI 10.1095/biolreprod.115.131615

Di-*n*-Butyl Phthalate Induces Multinucleated Germ Cells in the Rat Fetal Testis Through a Nonproliferative Mechanism[1]

Daniel J. Spade, Susan J. Hall, Shelby Wilson, and Kim Boekelheide[2]

Department of Pathology and Laboratory Medicine, Brown University, Providence, Rhode Island

ABSTRACT

In utero exposure to some phthalate esters adversely affects the development of the rat seminiferous cord, causing germ cell loss and increasing the number of multinucleated germ cells (MNGs). To understand the timing of MNG formation and determine whether it requires nuclear division, timed pregnant Sprague Dawley rats were exposed to 500 mg/kg di-*n*-butyl phthalate (DBP) or corn oil vehicle by oral gavage on Gestational Day (GD) 17 or 18 (0 h) and euthanized after 2, 4, 6, or 24 h or given a second dose at 24 h and euthanized 48 h after the initial dose. Dams were simultaneously exposed to 0.3 M 5-bromo-2′-deoxycitidine (BrdC; converted to 5-bromo-2′-deoxyuridylate [BrdU] in vivo) through a subcutaneous micro-osmotic pump implanted at −2 h. In the testes of male fetuses, DBP induced MNGs significantly beginning at 4–6 h and dramatically by 24 h when exposure began on GD 18 but not GD 17. Seminiferous cord diameter was significantly elevated in testes of rats treated with DBP at 24 and 48 h, and cell death, measured by TUNEL assay, was significantly elevated by DBP only at 48 h, when treatment began on GD 18. TUNEL-labeled MNGs were rare. Overall BrdU labeling rate in the testis was unaffected by DBP. Only one of 606 MNGs in BrdU-labeled sections had a strongly positive nucleus, confirming a non-proliferative mechanism of MNG formation, which is a degenerative process with the potential to adversely affect testis development.

fetal development, multinucleated germ cell, phthalate syndrome, testis

INTRODUCTION

In utero exposure to some phthalate esters (phthalates) disrupts the development of the fetal rat testis by adversely affecting multiple cell types, including the Leydig cells and the Sertoli and germ cells that make up the seminiferous cord. In Leydig cells, phthalates reduce testicular testosterone through a partially characterized mechanism involving decreases in steroidogenic gene transcription, leading to reproductive tract malformations [1–3]. In the fetal seminiferous cord, phthalates cause a dramatic increase in the rate of multinucleated germ cells (MNGs) [3–6] as well as loss of germ cells [6–8]. These effects on the fetal testis are the underlying cause of the hypothesized phthalate syndrome [9], which consists of early and later life-adverse outcomes for male reproductive tract development, including cryptorchid testis, hypospadias, and reduced sperm parameters. The similarity of these phthalate effects with the increased rates of hypospadias and cryptorchidism and the decreased sperm counts associated with testicular dysgenesis syndrome (TDS) in humans [10, 11] has led to the hypothesis that in utero exposure to environmental testicular toxicants, particularly phthalates, may contribute to testicular dysgenesis [9, 12]. This is an imperfect comparison, as germ cell cancers, which are a component of TDS, do not occur in rats generally or in phthalate-treated animal models, and TDS is believed to be the result of numerous factors, including genetic variants, lifestyle, and environmental exposures [11–14].

In the fetal testis, phthalates affect both Leydig cells and seminiferous cords. In many studies, pregnant rats are exposed to phthalates by oral gavage from mid- to late gestation, which leads to both Leydig cell and seminiferous cord effects in male fetuses [1–3, 5, 15–22]. However, studies of both human and mouse fetal testis indicate that the seminiferous cord effects of phthalates do not stem directly from their antiandrogenic activity, as phthalates alter the seminiferous cord even in the absence of a measureable antiandrogenic effect [4, 7, 23–29]. Due to a significant emphasis on the antiandrogenic outcomes of phthalates in the rat literature, seminiferous cord effects are relatively understudied. While apparent species differences exist in the sensitivity of the fetal testis to the antiandrogenic potency of phthalates [26–30], the rat fetal testis is an appropriate model to study the influence of phthalates on the human fetal seminiferous cord [8, 23].

MNGs are a hallmark of fetal phthalate exposure, but little is known about the mechanisms by which phthalates induce MNGs or the implications of MNGs for male reproductive health. It has been hypothesized that MNGs form by a proliferative mechanism and that the increase in MNGs following phthalate exposure is indicative of abnormal proliferative activity [3]. However, a short-term phthalate exposure during late gestation is sufficient to produce a significant increase in the rate of MNGs [6]. Further, MNGs form from differentiated germ cells, which are not proliferative [8, 31]. More likely than resulting from abnormal germ cell proliferation, MNG formation could be a degenerative process caused by a breakdown in intercellular bridges between fetal germ cells following loss of vimentin cytoskeletal projections in Sertoli cells and loss of Sertoli cell-germ cell contact [8, 15, 29]. This would ultimately result in the loss of those differentiated germ cells, as MNGs are lost through apoptosis in the early postnatal period [17, 22, 31].

We hypothesized that DBP exposure during a 48-h window in late gestation would lead to an increase in MNG formation

[1]This work was supported by the National Institute of Environmental Health Sciences at the National Institutes of Health (5R01ES017272-05 and 5T32ES007272-23) and the American Chemistry Council. This study was presented at the 54th Annual Meeting of the Society of Toxicology, 22–26 March 2015, San Diego, California, and in part at the Society of Environmental Toxicology and Chemistry North America 35th Annual Meeting, 9–13 November 2014, Vancouver, British Columbia, Canada.
[2]Correspondence: Kim Boekelheide, Department of Pathology and Laboratory Medicine, Brown University, Box G-E5, 70 Ship St., Providence, RI 02912. E-mail: kim_boekelheide@brown.edu

Received: 13 May 2015.
First decision: 24 June 2015.
Accepted: 18 September 2015.

eISSN: 1529-7268 http://www.biolreprod.org
ISSN: 0006-3363

TABLE 1. Sample size for each combination of gestational age, dose, and study time.

Study time (h)[a]	Treatment	Sample size
GD 17 Crl:CD (SD)[b]		
0–2	Corn oil	4
0–2	DBP	4
4–6	Corn oil	3
4–6	DBP	6
24	Corn oil	1
24	DBP	2
GD 18 Crl:SD[b]		
0–2	Corn oil	6
0–2	DBP	1
4–6	Corn oil	7
4–6	DBP	4
24	Corn oil	4
24	DBP	3
48	Corn oil	5
48	DBP	5

[a] Rats exposed to DBP for 0 or 2 h and 4 or 6 h were grouped together due to similarity of response.
[b] GD = gestational day, age of fetal rats at the time of first dose.

through a nonproliferative mechanism. To test this hypothesis, we utilized a unique exposure paradigm to capture proliferative activity throughout the entire DBP exposure window: pregnant rats (Gestational Day [GD] 17 or 18) were exposed to DBP by oral gavage while simultaneously receiving the proliferation marker 5-bromo-2′-deoxycitidine (BrdC), which is converted to 5-bromo-2′-deoxyuridylate (BrdU) in vivo, by subcutaneous osmotic pump. We analyzed the effects of DBP on cellular proliferation, cell death, seminiferous cord diameter, and MNG rate in the fetal testis 2–48 h after initiation of DBP exposure.

MATERIALS AND METHODS

Animals

Timed pregnant Sprague Dawley rats (Crl:CD [SD]), strain code 001, or Crl:SD, strain code 400 (total n = 55), were purchased from Charles River Laboratories (Wilmington, MA). Rats were housed in the Brown University animal care facility under controlled temperature (25–28°C) and humidity (30–70%) with a 12L:12D cycle and received Purina Rodent Chow 5010 (Farmer's Exchange, Framingham, MA) and water ad libitum. All animal care and use procedures were approved by the Brown University Institutional Animal Care and Use Committee in accordance with U.S. Public Health Service requirements and the *Guide for the Care and Use of Laboratory Animals* as well as the guidelines of the Society for the Study of Reproduction.

For 20 Crl:CD (SD) rats, treatment began on GD 17. For 35 Crl:SD rats, treatment began on GD 18. The day on which a vaginal plug was detected was designated as GD 0. Sample sizes for each treatment and time point are listed in Table 1. Osmotic pumps (Alzet, Cupertino, CA) were filled with 0.3 M BrdC (MP Biomedicals, Santa Ana, CA) in sterile-filtered (0.22 μm) PBS (BBL FTA Hemagglutination Buffer; Becton Dickinson and Company, Franklin Lakes, NJ) and primed by incubating overnight in sterile PBS in a 37°C water bath. Pregnant dams were anesthetized using 2–3% isoflurane (Henry Schein Animal Health, Dublin, OH), and pumps were implanted subcutaneously through a dorsal skin incision 2 h prior to initiation of dosing. BrdC is converted to BrdU in vivo and has a greater aqueous solubility than BrdU [32]. Rats were given 500 mg DBP/kg body weight or corn oil vehicle in a 1-ml/kg body weight dosing solution by oral gavage. Doses were administered at 0 h for all animals and at 24 h for those animals in the 48-h time point. The 500-mg/kg dose and late gestation timing of administration were chosen based on the consistent induction of MNGs by this dose in multiple studies [3, 4, 15–17, 22], including a short exposure from GD 19 to GD 20 in Wistar rats [6]. Rats were euthanized by inhalation of isoflurane at 0, 2, 4, 6, 24, or 48 h relative to the initial dose. The uterus was removed, and all fetuses were collected, weighed on an analytical balance, and immediately euthanized by decapitation. The uterine position and weight of each fetus was recorded. Fetuses were retained on ice in Hanks Balanced Salt Solution without calcium, magnesium, or phenol red (Gibco/Life Technologies, Grand Island, NY, or Corning/Mediatech, Manassas, VA) and dissected under a Zeiss Discovery.V8 or Nikon SMZ-U stereomicroscope. Sex was determined for each fetus by microscopic investigation of the fetal gonad. One testis was collected from each male fetus and fixed in Modified Davidson Solution (Electron Microscopy Sciences, Hatfield, PA) for 15 min, then transferred to 70% ethanol and held at 4°C until further processing. In most cases, one testis was collected from each of four fetuses from each litter, but the number of male fetuses per litter ranged from 2 to 12 with a mean ± SEM of 5.3 ± 0.27 and mode of four.

Histology and Immunohistochemistry

Fixed testes were dehydrated through a series of ethanols and xylenes on a Triangle Biomedical Sciences ATP/1 processor, embedded in paraffin, and cut at 5 μm in four-section series. Within each four-section series, sections 1 and 3 were stained with hematoxylin and eosin (H&E). Section 2 was used for immunohistochemistry (IHC), and section 4 was used as an IHC negative control, which received no primary antibody or no TdT enzyme in TUNEL assays. Prior to IHC labeling, slides were deparaffinized in xylenes and rehydrated through a series of ethanols to PBS. For BrdU IHC labeling, endogenous peroxidase was blocked with 4.5% H_2O_2 diluted in methanol (both obtained from Fisher Chemical, Pittsburgh, PA) for 10 min, sections were permeabilized for 5 min in PBS with 0.1% Triton X-100 (Sigma-Aldrich, St. Louis, MO), and antigen retrieval was performed in 10 mM citrate buffer pH 6.0 heated in a vegetable steamer for 20 min, followed by 20 min at room temperature. Histone extraction in HCl was performed based on the method described by Bak and Panos [33]. Nonspecific staining was blocked using BLOXALL Blocking Solution (Vector Laboratories, Burlingame, CA) for 10 min and then a blocking buffer consisting of PBS with 1% w/v bovine serum albumin and 5% v/v normal goat serum (both from Sigma-Aldrich) for 30 min. Sections were incubated with anti-BrdU primary antibody (clone Bu20a, product no. M0744; DAKO, Carpinteria, CA) at a 1:100 dilution in blocking buffer or with blocking buffer alone overnight at 4°C in a humidified chamber. All sections were incubated for 90 min at room temperature with goat-anti-mouse IgG secondary antibody (product no. B0529; Sigma-Aldrich) diluted 1:200 in blocking buffer. Avidin-biotin peroxidase conjugation was performed using the Vectastain ABC Elite kit (Vector Laboratories), and peroxidase staining was developed using 3,3′-diaminobenzidine (DAB; Vector Laboratories) as the substrate. Slides were counterstained with hematoxylin, Gill no. 3 (Sigma-Aldrich). TUNEL labeling was performed using the Apoptag Peroxidase In Situ Apoptosis Detection Kit (EMD Millipore, Billerica, MA) according to the manufacturer's protocol, with the following modifications: the endogenous peroxidase blocking step was omitted, the chromogenic reaction was performed using DAB from Vector Laboratories, and sections were counterstained with hematoxylin. All sections were cleared with isopropanol and Fisherbrand Citrisolv Clearing Agent (Thermo Fisher Scientific, Waltham, MA) and mounted using Cytoseal-60 (Thermo Fisher Scientific).

Morphology Quantification

Slides were examined on an Olympus BH-2 light microscope for quality of histology and specificity of staining and then scanned at 40× on an Aperio ScanScope CS (Leica Microsystems Inc., Buffalo Grove, IL). BrdU-positive cells were quantified using a nuclear IHC counting algorithm within Leica ImageScope software. TUNEL-positive cells within seminiferous cords were counted manually on scanned slides in ImageScope. TUNEL-stained slides were also used to quantify the seminiferous cord diameter by measuring the diameter of the minor axis for each seminiferous cord in ImageScope. BrdU-labeled slides were used to count MNGs. All putative MNGs were hand checked on the light microscope, and the adjacent H&E sections were used for confirmation when possible. MNGs were not quantified on the TUNEL-stained slides, but notes of any TUNEL-positive MNGs were recorded. Finally, a morphometric analysis of TUNEL-labeled slides was performed in ImageJ using an automatic thresholding procedure to approximate the proportion of cross-sectional area occupied by the low-cell-density interstitium often located in the center of rat fetal testis cross sections, relative to the total area, which includes seminiferous cords, highly cellular interstitium, and tunica. This estimate was performed through a conversion of raw images to binary black-and-white images using the IsoData algorithm in Image J, based on the method of iterative intermeans [34]. The estimated area of nuclei within the interstitial area, identified as dark spots between 0 and 25 μm^2, was added to the total light interstitial area. The area occupied by blood vessels, which appear white in the binary image, was subtracted from the total light interstitial area. Blood vessel area was estimated as the sum of light objects with area of 300–5000 μm^2 and circularity values of 0.05–1.00.

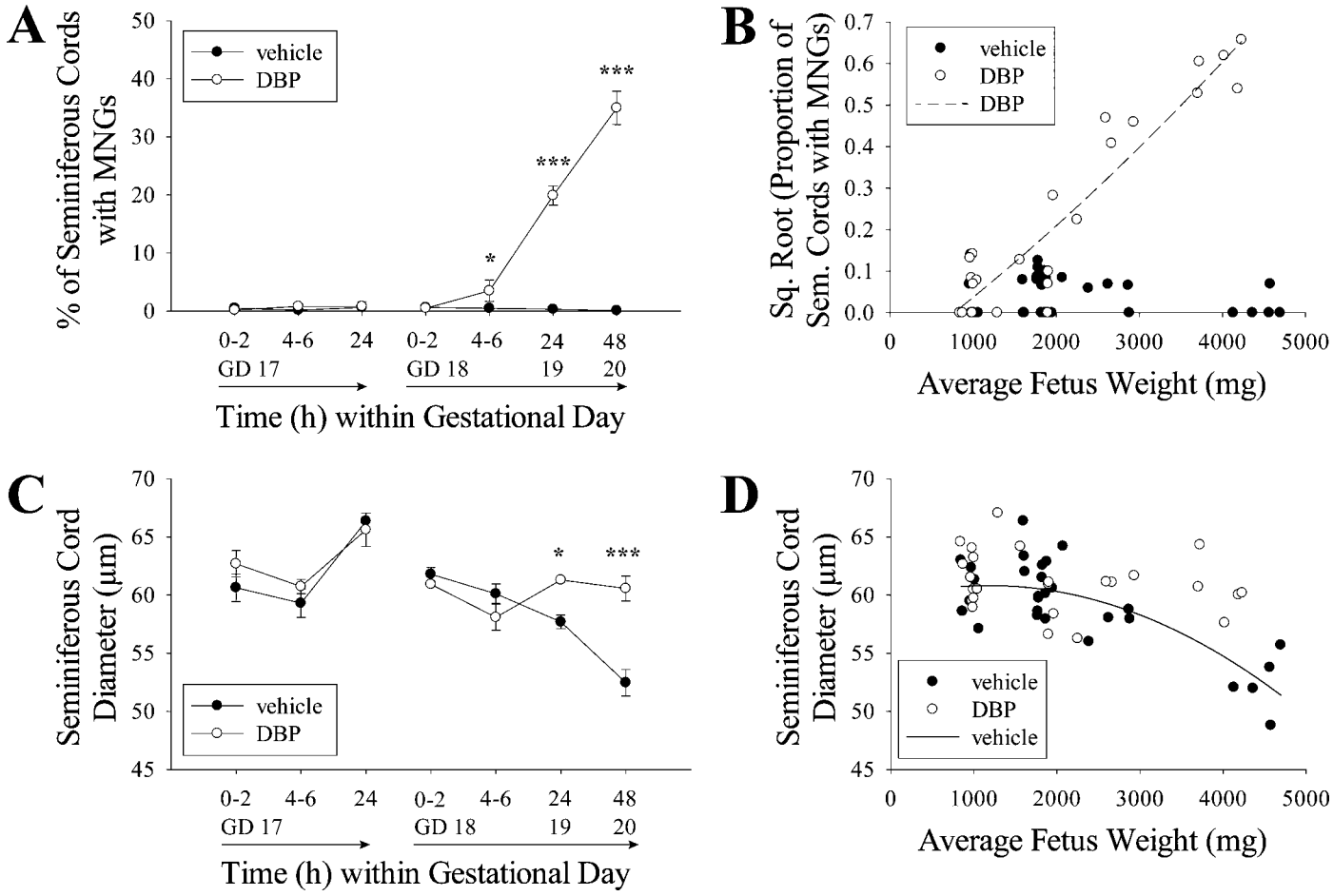

FIG. 1. DBP alters fetal testis morphology. DBP treatment did not increase the frequency of MNGs when treatment began on GD 17, but DBP significantly increased MNG frequency in rat fetal testis within 4–6 h when treatment began on GD 18 (**A**). The square root-transformed proportion of tubules with MNGs increased relative to fetus weight according to a quadratic trend ($n = 25$, $R^2 = 0.8837$, $P < 0.0001$); while the vehicle-treated testis MNG frequency data passed the normality and equal variance assumptions for quadratic regression, the fit against fetus weight was not significant ($n = 30$, $R^2 = 0.1263$, $P = 0.1616$) (**B**). DBP treatment did not significantly alter the seminiferous cord diameter when treatment began on GD 17, but when treatment began on GD 18, seminiferous cord diameter was significantly higher in DBP-treated than vehicle-treated testes at 24 and 48 h (**C**). When analyzed by fetus weight, seminiferous cord diameter (**D**) in vehicle-treated samples decreased according to a quadratic trend ($n = 30$, $R^2 = 0.6104$, $P < 0.0001$), while DBP-treated samples ($n = 25$) did not significantly fit any linear ($R^2 = 0.0566$, $P = 0.2522$) or quadratic ($R^2 = 0.0843$, $P = 0.3794$) relationship with fetus weight and showed no obvious decrease in diameter. To correct for nonnormal distribution, MNG data were converted to proportions and square root transformed, and transformed data were used for ANOVA and regression analyses. All pairwise comparisons were made by two-way ANOVA followed by the Holm-Sidak test (*$P < 0.05$, ***$P < 0.001$). Values in **A** and **C** are mean ± SEM.

Data Analysis and Statistics

All data were quantified at the level of the fetus. The arithmetic mean of values from all fetuses in the same litter was used as the value for data analysis so that the litter was treated as the unit of replication. For most litters, the number of fetuses to be analyzed was limited to four, but for all litters, the range was two to eight fetuses, with a mode of four and mean ± SEM of 3.98 ± 0.15. A total of 219 testes (219 unique fetuses) from the 55 litters were analyzed. For the morphometric analysis only, TUNEL sections with imperfections were excluded, leaving 185 fully intact sections in the analysis (from 185 fetuses), including at least one from each litter, for a sample size of $n = 55$. Due to similarity of responses and small sample sizes in early time points, the 0- and 2-h and 4- and 6-h time points were combined for statistical purposes. Linear, quadratic, and exponential regression analyses were performed as appropriate to show the strength of association between end-point data and fetal weight. Statistical comparisons by treatment and time point were performed using two-way ANOVA, followed by the Holm-Sidak post hoc test for multiple comparisons. MNG data for GD 17 and GD 18 rats and percent interstitial area data for GD 18 rats were not normally distributed. To correct for this, the proportion of seminiferous cords with MNGs was square root transformed, and percent interstitial area data were $\log_{10}$ transformed. TUNEL data for GD 18 rats did not have equal variance. To correct for this, the percent of seminiferous cords with TUNEL-positive cells was $\log_{10}$ transformed. These transformations produced normally distributed data with equal variance, and regression and two-way ANOVAs were performed on the resulting data as appropriate. All statistical analyses were performed using SigmaPlot (Systat Software, San Jose, CA).

RESULTS

Short-Term DBP Exposure Impairs Late Gestational Development of the Rat Seminiferous Cord

DBP exposure had significant effects on the morphology of the seminiferous cords within 24 h of initial exposure, but only when the exposure began on GD 18, not GD 17 (Fig. 1). In fetal rats exposed to DBP on GD 18 and 19, there was a significant increase in MNG frequency beginning by 4–6 h of exposure. The difference was highly significant at both 24 and 48 h (Fig. 1A). Notably, the relationship between average fetus weight and experiment time was linear for both rats exposed beginning on GD 17 ($n = 20$, $R^2 = 0.8788$, $P < 0.0001$) and on GD 18 ($n = 35$, $R^2 = 0.9488$, $P < 0.0001$), including both DBP- and vehicle-treated rats (Supplemental Figure S1; Supplemental Data are available online at www.biolreprod.

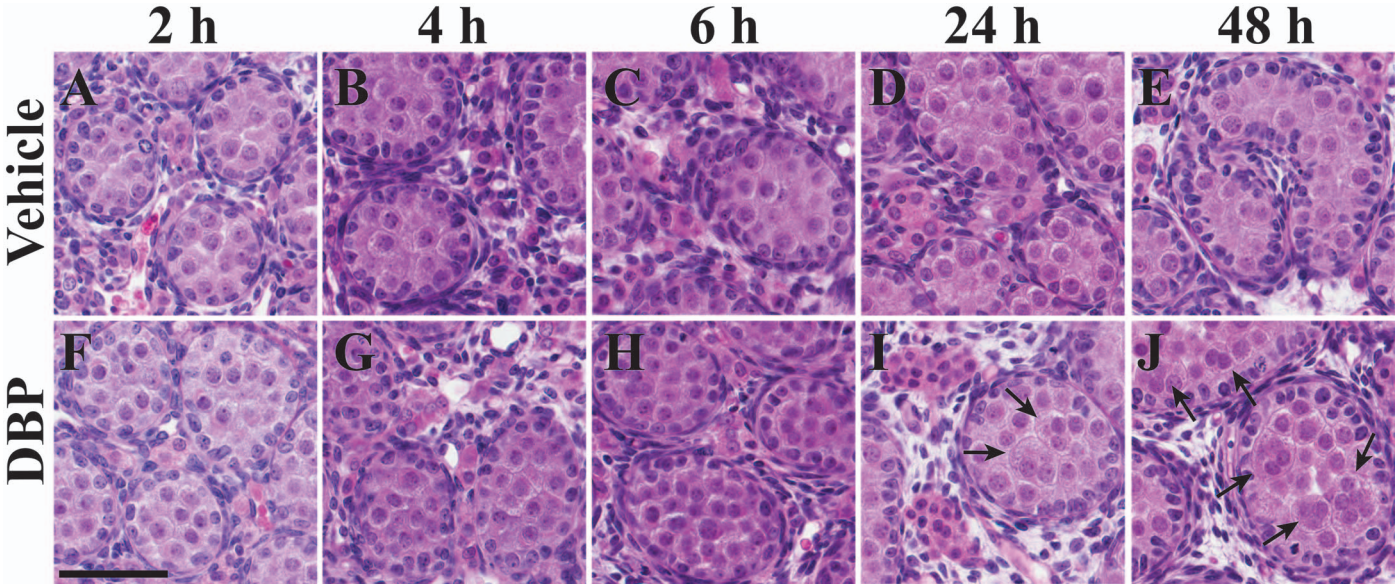

FIG. 2. Representative images of GD 18–20 testis. Representative images of rat fetal testes from animals exposed to vehicle (**A**–**E**) or DBP (**F**–**J**) beginning on GD 18 and collected 2, 4, 6, 24, or 48 h after the initial dose. MNGs were much more frequent, and average seminiferous cord diameter was higher in DBP-treated testes at 24–48 h. These trends are visible in **I** and **J** relative to **D** and **E**. Arrows indicate MNGs. Bar = 60 μm.

org), making fetus weight a good proxy for gestational age (Supplemental Figure S1). Utilizing this proxy, when square root-transformed data for the proportion of seminiferous cords with MNGs in DBP-exposed testes (both GD 17 and 18) were plotted by fetus weight, they increased according to a quadratic trend (Fig. 1B; n = 25, $R^2 = 0.8837$, $P < 0.0001$). This temporally coincided with the seminiferous cord diameter in vehicle-treated fetuses decreasing throughout the exposure period according to a quadratic fit ($R^2 = 0.6104$, $P < 0.0001$), with a dramatic decrease around GD 20, while DBP-exposed rats showed no such decrease (Fig. 1, C and D). Representative images of testes exposed to vehicle or DBP beginning on GD 18 are shown in Figure 2, with the increased seminiferous cord diameter and MNG rate visible at 24–48 h of DBP exposure.

Cell Death and Proliferation Following Late Gestational DBP Exposure

The pattern of TUNEL staining (Fig. 3) was similar to previous reports in the rat fetal testis, with infrequent labeling during late gestation and no obvious staining in Sertoli cells [35]. The overall rate of cell death in the seminiferous cord, measured by TUNEL, decreased with gestational age (Fig. 3A) or fetal weight (Fig. 3B), counting all visible signals, including small or faint signals likely indicating the late stages of apoptosis. This indicated that the rate of germ cell apoptosis decreased dramatically at approximately GD 17–18. The trend in vehicle-treated samples was significant (two-parameter exponential decay fit; n = 30, $R^2 = 0.7177$, $P < 0.0001$). TUNEL data from DBP-treated testes on GD 17 and 18 combined were not normally distributed even after $\log_{10}$ transformation, so they could not be used for regression analysis, but they showed a negative association with fetus weight also. DBP treatment did not significantly influence the rate of cell death, measured by TUNEL, in the seminiferous cords when treatment began on GD 17, but there was a significantly higher rate of TUNEL signal in the DBP-exposed than in the vehicle-exposed testes of GD 18 rats at 48 h only (Fig. 3A). Widespread apoptotic death of MNGs was not observed at any time point, though MNGs with TUNEL-positive nuclei were observed infrequently (Fig. 3, D and H).

Specific labeling of proliferative nuclei by the BrdU antibody has been previously reported [36], and we have used it to identify proliferative cells in the adult rat testis [37]. In the current study, proliferative activity occurred almost exclusively in somatic cells, with Sertoli cells becoming nearly universally labeled by 48 h of BrdC exposure beginning on GD 18. In addition to Sertoli cells, BrdU labeling was frequent in peritubular cells, tunica cells, and some interstitial cells but was infrequent in Leydig cells (based on morphology) and germ cells (Fig. 4 and Supplemental Figure S2), as expected for this developmental age [16, 35]. Also as expected, BrdU labeling frequency increased with increasing time of exposure to BrdC (Supplemental Figure S2). DBP had no effect on proliferation as measured by the proportion of BrdU-positive nuclei of all testicular cell types in histological sections when treatment began on GD 17 (Fig. 4A) or GD 18 (Fig. 4B), but BrdU labeling rate increased according to a quadratic fit in both vehicle- (n = 30, $R^2 = 0.8307$, $P < 0.0001$) and DBP-treated (n = 25, $R^2 = 0.8574$, $P < 0.0001$) testes (Fig. 4C). Of 606 MNGs counted in the study, only two were BrdU positive, with one showing a faint signal and a second displaying a strongly BrdU-positive nucleus; the latter cell had at least five identifiable nuclei in the BrdU-stained section, only one of which was BrdU positive (Fig. 4H).

Overall Testis Morphometry in Late Gestation

Whole mounted cross sections of fetal testis often contain a large centrally located area of low-cell-density interstitial tissue. Given the significant changes in seminiferous cord diameter measured in this study (Fig. 1) and the previously reported reduction in the number of seminiferous cord cross sections in the testis following DBP exposure [15], in addition to the Leydig cell clustering caused by phthalates [38, 39], both of which effects are unique to phthalates among testicular toxicants, we hypothesized that the area occupied by this low-cell-density interstitial space might also change with developmental age and be altered by DBP exposure. When automatic

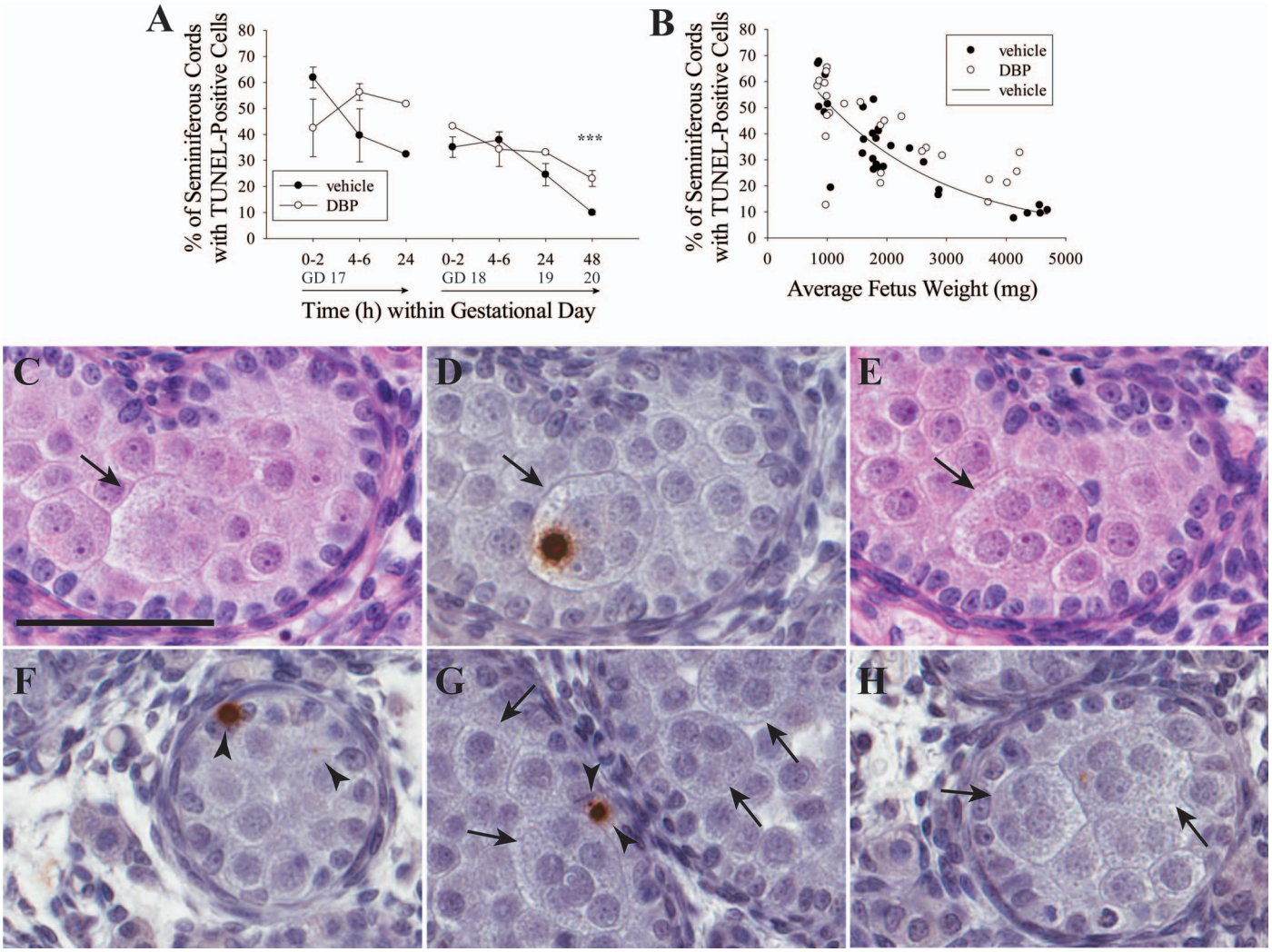

FIG. 3. DBP has no effect on apoptosis at most time points, but it is the probable mechanism of MNG loss. DBP treatment did not increase the frequency of TUNEL-positive cells significantly in the rat fetal testis when treatment began on GD 17 but significantly increased apoptosis rate in GD 18 rats after 48 h (***$P < 0.001$) (**A**). GD 18 data but not GD 17 had unequal variance. To correct for this, GD 18 data were $\log_{10}$ transformed, and then data were analyzed by two-way ANOVA followed by the Holm-Sidak test. Only the interaction term was significant for GD 17 rats ($P = 0.038$). Values in **A** are mean ± SEM. When all samples were analyzed by fetus weight (**B**), the frequency of seminiferous cords with TUNEL-positive cells in vehicle-treated fetal rat testis decreased according to a two-parameter exponential fit ($n = 30$, $R^2 = 0.7177$, $P < 0.0001$). The combined GD 17 and 18 data for DBP-exposed rats was not normally distributed and could not be corrected using a transformation. Therefore, it was not subjected to regression analysis, but the overall trend was downward with increasing fetal weight. **C**–**E**) Three serial 5-μm sections from a rat treated with DBP for 48 h beginning on GD 18, stained with H&E (**C**, **E**) or TUNEL with hematoxylin counterstain (**D**). An MNG is visible in all three sections (**C**–**E**) with a single TUNEL-labeled nucleus in **D**. **F**) Representative TUNEL-positive cells in a sample treated with vehicle for 48 h starting on GD 18, demonstrating the range of signal size and strength in the study. In **G**, several TUNEL-negative MNGs are shown in a sample treated for 48 h with DBP beginning on GD 18. **H** shows an MNG with a weak TUNEL signal. In all panels, arrows indicate MNGs, and arrowheads indicate TUNEL-positive cells. Bar = 60μm.

thresholding was used to separate the light and dark cellular area in scanned images (Fig. 5), the white space, comprised primarily of this low-cell-density interstitial area, ranged from 3.590% to 29.084% of the cross-sectional area with a mean ± SEM of 12.476 ± 0.839. The $\log_{10}$-transformed percent of cross-sectional area increased on average with increasing fetus weight in testes from both vehicle- ($n = 30$, $R^2 = 0.3162$, $P = 0.0012$) and DBP-treated ($n = 25$, $R^2 = 0.5145$, $P < 0.0001$) rats (Fig. 5F). This was a highly variable measurement but showed a rough increase on average with fetus weight. Within fetuses treated beginning on GD 17, $\log_{10}$(% interstitial area) was significantly lower in DBP-treated than vehicle-treated testes at 4–6 h ($P = 0.005$). There was no statistically significant difference between DBP- and vehicle-treated samples when treatment began on GD 18 (Fig. 5E).

DISCUSSION

Changing Context of Fetal Testis Morphology

Gonocytes in the fetal mammalian testis develop asynchronously through three phases, giving rise to the population of cells that will become spermatogonial stem cells (reviewed in Culty [40] and Culty [41]). First, the gonocyte population undergoes mitotic expansion. Next, in late gestation, on approximately GD 18 in the rat, gonocytes become quiescent before finally entering a transitional phase. The transitional phase is characterized by the differentiation of gonocytes into spermatogonia and the migration of germ cells from the center of the seminiferous cord to the basement membrane of the developing seminiferous tubule. Germ cell apoptosis is frequent during the mitotic stage but very infrequent from the

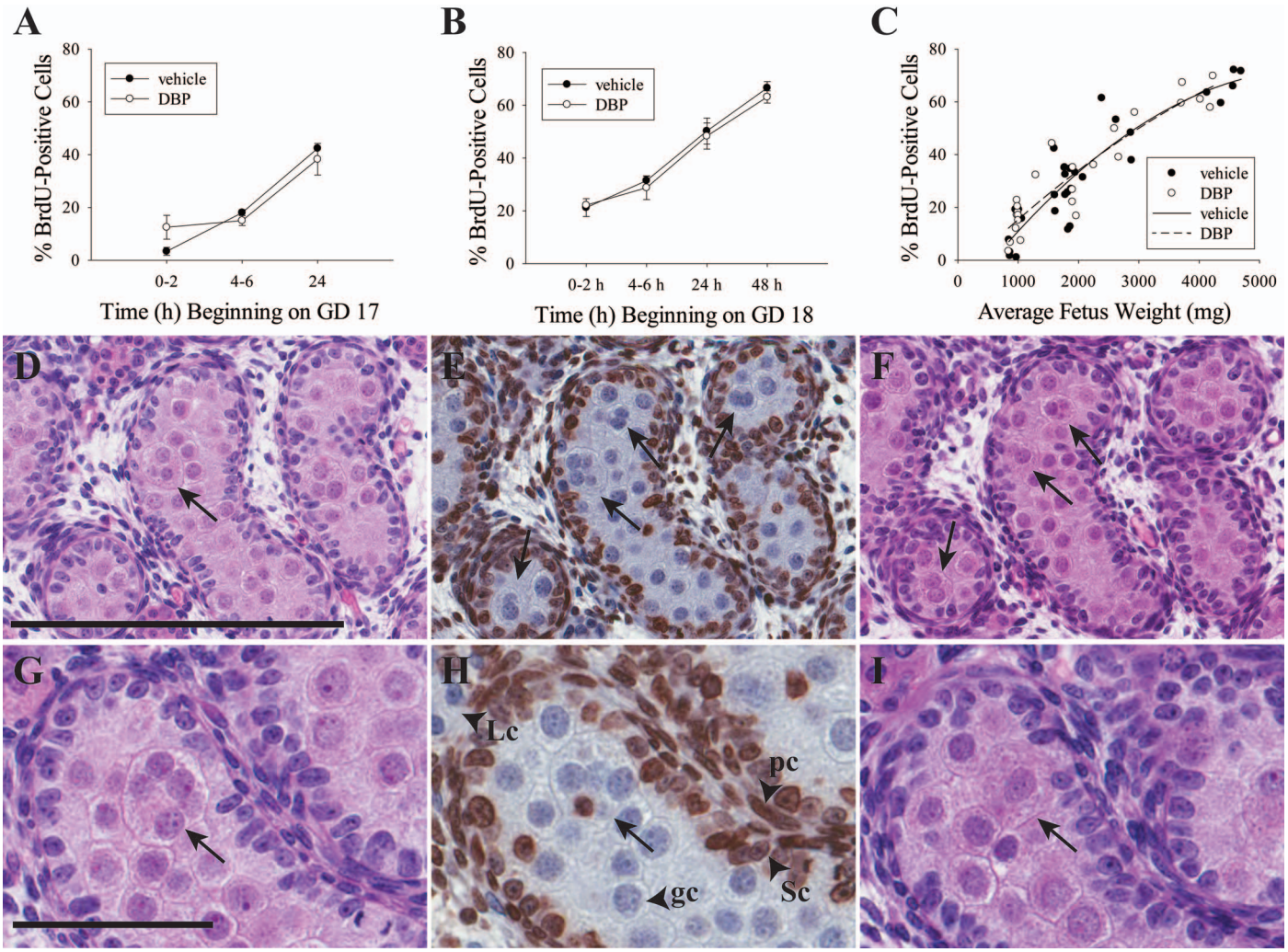

FIG. 4. MNGs do not form by a proliferative mechanism. DBP treatment did not increase or decrease the frequency of BrdU-positive cells in the rat fetal testis when treatment began on GD 17 (**A**) or GD 18 (**B**). These values are shown in separate panels because each panel has a different start time for BrdU exposure on GD 17 and GD 18, respectively. Values in **A** and **B** are mean ± SEM. Data analyzed by two-way ANOVA followed by the Holm-Sidak test. While there were no differences by treatment within time point, the time factor was significant ($P < 0.001$) for GD 17 and GD 18 rats. When all samples were analyzed by fetus weight (**C**), the frequency of seminiferous cords with BrdU-positive cells in both vehicle- and DBP-treated fetal rat testis increased according to a quadratic trend (DBP: $n = 25$, $R^2 = 0.8574$, $P < 0.0001$; vehicle: $n = 30$, $R^2 = 0.8307$, $P < 0.0001$). **D–F**) Three serial 5-μm sections from a rat treated with DBP for 48 h beginning on GD 18, stained with H&E (**D**, **F**) or by IHC for BrdU with hematoxylin counterstain (**E**). Four MNGs are clearly visible in the BrdU-labeled section (all are BrdU negative). One is visible on the adjacent section **D**, while three are also visible on adjacent section **F**. A similar series of three 5-μm sections is shown in **G–I**, with an MNG visible in all three sections that has a single BrdU-labeled nucleus in **H**. In all panels, arrows indicate MNGs. Labeled arrowheads in **H** demonstrate normal pattern of BrdU staining in peritubular cells (pc) and Sertoli cells (Sc) but not in germ cells (gc) or Leydig cells (Lc). Bar in **D** = 200 μm for **D–F**, and bar in **G** = 60 μm for **G–I**.

quiescent stage until a wave of spermatogonial apoptosis that takes place after birth. Phthalate exposure during fetal life significantly perturbs the normal process of testis development. The changing number and types of fetal germ cells present during testis development create a moving baseline that must be taken into account to understand phthalate effects during specific windows of fetal development.

In this study, we sought to understand how MNGs formed in response to DBP exposure, how critical the timing of exposure was for MNG formation, and whether loss of MNGs by apoptosis would begin shortly after their appearance. A key finding was that the morphology of the testis changed dramatically during the window of exposure when MNGs are formed and that this process was temporally linked to the susceptibility of the fetal rat testis to DBP-induced MNG formation. The testes of fetal rats treated with corn oil vehicle in this study displayed several morphological changes with fetus weight, including a decrease in seminiferous cord diameter (Fig. 1D). This decrease occurred rapidly at approximately GD 20, which corresponds with the reported increase in number of seminiferous cord cross sections on GD 20–21 in vehicle-treated rats in a previous study [15, 16]. During the same time frame, evidence of apoptosis in the seminiferous cords decreased (Fig. 3B), while evidence of proliferation across the whole testis increased (Fig. 4C). However, proliferative activity was limited almost exclusively to somatic cells (Fig. 4 and Supplemental Figure S2), as would be expected given that late gestation is a time of fetal growth but germ cell quiescence. We used image analysis of testis sections to produce an integrated measurement for the changes in fetal testis morphology during development, based on the proportion of the section comprised of low-cell-density interstitial area (Fig. 5). This was highly variable due in part to the multifactorial nature of trying to capture seminiferous

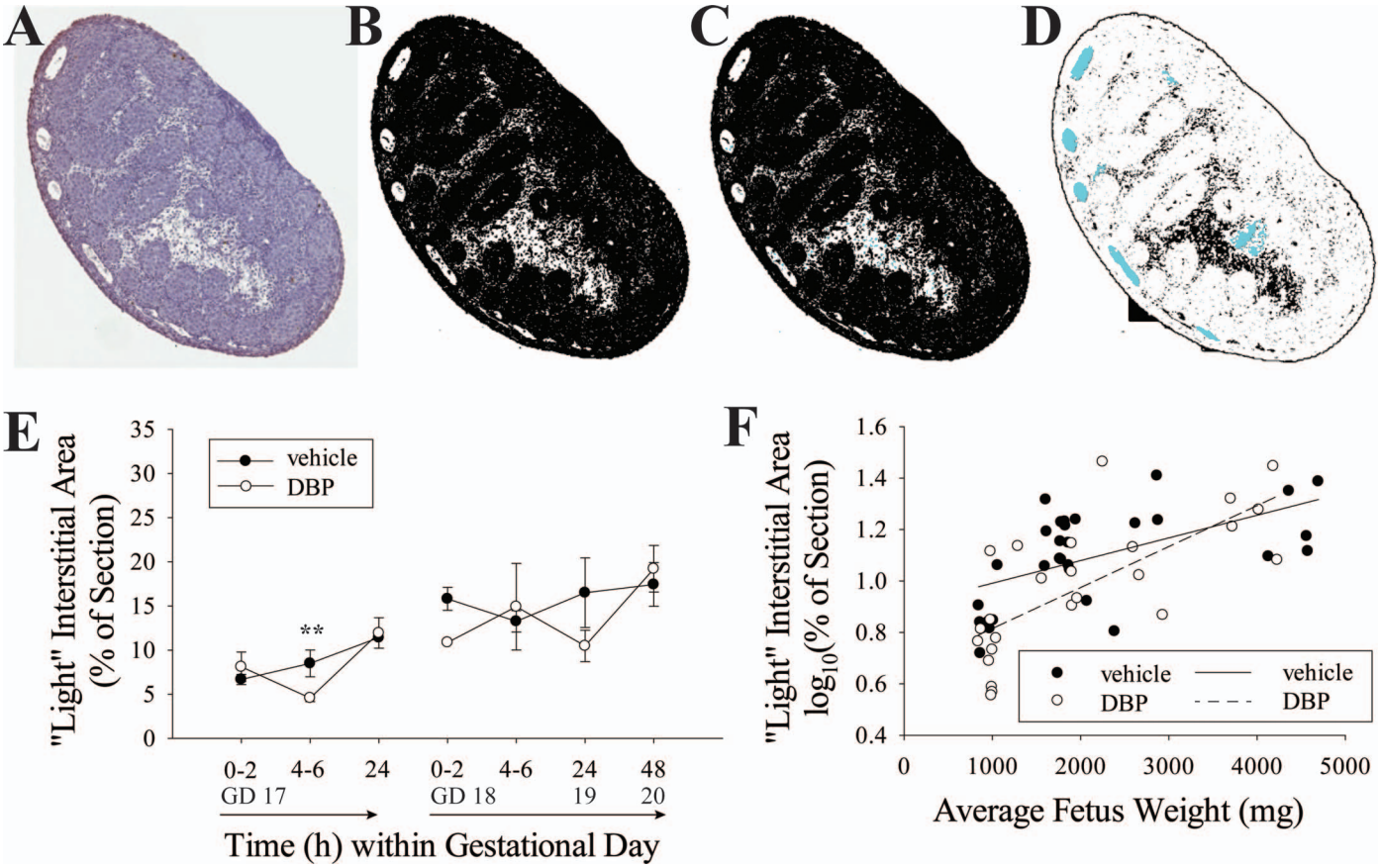

FIG. 5. The low-cell-density interstitial area in the testis increases with gestational age. **A**–**D**) The conversion of a whole-mounted testis section stained with TUNEL assay and hematoxylin counterstain (**A**) to a binary black-and-white image where the white area largely represents low-cell-density interstitial area (**B**). In **C**, the nuclear area within the interstitium (blue) is identified and added to the interstitial total area. In **D**, blood vessel area (blue), which also appears as white in the binary images, is subtracted from the interstitial area. GD 17 data but not GD 18 were not normally distributed. To correct for this, GD 18 data were $\log_{10}$ transformed, and then data were analyzed by two-way ANOVA followed by the Holm-Sidak test. The light-colored, low-cell-density interstitial area in the cross sections did not differ significantly by treatment group when GD 18 data were analyzed by two-way ANOVA (**D**); however, at 4–6 h of treatment beginning on GD 17, the $\log_{10}$-transformed interstitial area was greater in vehicle- than DBP-treated samples (**$P = 0.005$). Values in **E** are mean ± SEM. For regression analysis, all data were $\log_{10}$ transformed to correct for nonnormal distribution. $\log_{10}$-transformed interstitial area, as percent of the section, slightly increased with fetus weight in both vehicle- (n = 30, $R^2 = 0.3162$, $P = 0.0012$) and DBP-treated (n = 25, $R^2 = 0.5145$, $P < 0.0001$) groups (**F**).

cord diameter, number of cords, and other variables. Also, this is likely subject to variability in the depth at which sections were obtained. While this analysis did not show a consistent difference between DBP- and vehicle-treated testes, it did indicate that the average interstitial area increases slightly throughout the time window of our study. Further development of this analysis may be useful to investigate whether this ratio is altered by exposure to other toxicants that adversely affect fetal testicular development.

DBP Alters the Morphology of the Seminiferous Cord

Given that dramatic morphogenetic changes in the seminiferous cord coincide with the timing of vulnerability to phthalate-induced MNG induction, we hypothesize that MNGs induced by fetal phthalate exposure are precipitated by phthalate-driven disruption of normal developmental processes in the seminiferous cords. The increase in MNGs in rats exposed to DBP beginning on GD 18 was statistically significant after only 4–6 h of DBP exposure (Fig. 1A). This is consistent with the window of susceptibility reported in two studies in which DBP exposure on GD 19 and 20 was sufficient to cause an increase in MNGs [6] and germ cell aggregation [42]. DBP has been previously reported to increase seminiferous cord diameter [4], but our data indicate that this difference results from a failure of the seminiferous cord to decrease in diameter at approximately GD 19–20 as in vehicle-treated rats (Figs. 1 and 2). The timing of this event also coincided with the increase in the number of seminiferous cord cross sections per rat fetal testis, which is reduced by DBP doses as low as 50 mg/kg/day [15, 16]. Therefore, the normal maturation of the rat testis in the final days of gestation is characterized by a greater number of visible seminiferous cords in testis cross sections that are smaller in diameter, possibly caused by rapid convolution of seminiferous cords. This morphogenetic process is susceptible to the adverse effects of phthalate exposure.

DBP exposure did not change the rate of proliferation in the testis or rate of cell death in the seminiferous cords at most time points (Figs. 3 and 4), consistent with the exposure window coinciding with germ cell quiescence, which occurs from approximately GD 18 to Postnatal Day (PND) 3 in the rat [41]. During this time of fetal testicular growth, cell death in seminiferous cords was low (Fig. 3). Conversely, overall cell proliferation in the testis was high (Fig. 4 and Supplemental Figure S2), driven almost entirely by testicular somatic cells. These observations are consistent with the previously reported maximum germ cell death at GD 15–16 and low TUNEL

staining after GD 18 [35], germ cell proliferation that is frequent prior to GD 18 but infrequent from GD 18 to PND 2–3, a high rate of Sertoli cell proliferation at GD 20, and a low rate of fetal Leydig cell proliferation in late gestation [15, 16, 35]. DBP perturbed this pattern only by increasing TUNEL staining at GD 18, similar to one study of mono-(2-ethylhexyl) phthalate, a compound with similar effects to DBP, in the mouse fetal testis in vitro [7]. In the previous DBP study, we also found a significant reduction in BrdU labeling across testicular cell types in DBP-treated testes on GD 17, 20, and 21 [16]. This discrepancy in the effect of DBP exposure on cell proliferation in the fetal testis could have resulted from the longer duration of exposure in the previous study, where treatment began at GD 12. Overall, however, our results indicate that DBP alters the morphology of the fetal seminiferous cord without having profound effects on testicular cell proliferation or cell death.

Phthalate-Induced Fetal Testicular MNGs Are Nonproliferative

The most critical finding in the present study was the confirmation that MNGs form through a mechanism that does not rely on germ cell proliferation, implying that MNGs are a degenerative feature of the response to phthalates. While this finding contradicts one report that MNGs were sometimes IHC positive for proliferating cell nuclear antigen (PCNA) [3], it is in accord with our previous findings of DBP leading to no change or a decrease in proliferative activity across all fetal testicular cell types, no evidence of proliferation in MNGs following DBP exposure, and that PCNA staining in MNGs may have been influenced by fixation-related nonspecific staining patterns [15, 16]. The present study improved on this line of inquiry by using continuous BrdC exposure beginning prior to dosing with DBP. Continuous BrdC exposure was a sensitive way to detect evidence of a proliferative mechanism of MNG formation if it occurred, especially given that the rate of BrdU labeling across the whole testis increased dramatically concurrent with the significant increase in MNGs (Fig. 4 and Supplemental Figure S1). The present result is also consistent with reports that MNGs are formed from differentiated germ cells, which are not proliferative [8, 31]. It previously has been reported in addition to MNGs that phthalates produced histological evidence of atypical germ cell mitosis in fetal rats on PND 3 and 7 [17]. While it is possible that DBP exposure in utero could lead to abnormal germ cell proliferation in early postnatal life, our data do not indicate that this aberrant mitotic activity begins in utero or that it is related to induction of MNGs through a proliferative mechanism.

MNGs, notably, are induced by numerous toxicants, physical stressors, and genetic factors affecting spermatogenesis in adult rodent testes, in which context they are typically called multinucleated giant cells [43–47], and are also found in cryptorchid testis in humans [48]. Adjacent testicular germ cells are connected at various stages in both fetal and adult life by intercellular bridges made up of proteins including testis expressed 14 (TEX14) [49–51]. MNGs may form by the collapse of these intercellular bridges, as evidenced by the production of MNGs in adult rat testis following cytochalasin D treatment and loss of actin filaments [52]. Additionally, unique sphingolipids are required for germ cell bridge formation, and loss of these sphingolipids by knockout of ceramide synthase 3 leads to increased rates of MNGs and increased germ cell intercellular bridge diameter labeled by TEX14 in the mouse [53]. It is plausible that MNGs in the fetal testis form through a similar process of intercellular bridge collapse following DBP exposure. Our present results strongly support this hypothesis, clearly indicating that MNGs in the fetal testis are nonproliferative and are induced rapidly as a result of phthalate treatment when germ cells are quiescent.

In a previous study, exposure of human fetal testis xenografts to DBP resulted in altered expression of genes related to the actin filament and to organelle localization, which suggests that DBP causes testis pathology by altering cytoskeletal components of testicular cells [24]. This is further supported by evidence from fetal rats that phthalate exposure leads to altered localization of vimentin in the cytoskeleton of Sertoli cells, retraction of the Sertoli cell processes that surround germ cells, and disrupted expression of cell adhesion molecules and contacts between Sertoli and germ cells [15]. Further, the timing of MNG formation is consistent with this hypothesis. Germ cell bridges appear in transitional and late gestational germ cells in humans [54, 55], rats [56], and mice [49], all of which are susceptible to phthalate-induced MNGs [23, 29].

Phthalates and Germ Cell Loss

We found no evidence that widespread loss of MNGs due to DBP exposure occurred during the window of GD 17–20, consistent with previously published data on loss of MNGs and germ cell apoptosis [15–17, 22, 31]. Further, there was no evidence of an altered rate of apoptosis in the DBP-exposed seminiferous cords until PND 20 (Fig. 3A; 48 h), consistent with the quiescent window for rat germ cells from GD 18 to PND 2–3 [41]. Postnatal germ cell apoptosis begins between PND 1 and PND 6 [16, 35, 56, 57], and a significant wave of germ cell apoptosis occurs on PND 15–20 [58]. Given that MNGs are not lost shortly after forming, the majority of MNGs presumably are lost through apoptosis when it becomes frequent during postnatal life, between PND 4–7 and PND 10–16 in the rat [17, 22] or by PND 7 in the mouse [31]. Apoptosis as the ultimate mechanism of MNG loss is likely. Not only does MNG loss coincide with the timing of elevated levels of germ cell apoptosis, but in the present study, we observed at least one MNG with an apoptotic nucleus (Fig. 3). Further, we previously found that DBP-induced MNGs are more frequent and that abnormal germ cells are more persistent in adult mice lacking *Tp53* [31].

As phthalate-induced MNGs appear temporarily and are lost postnatally, germ cell loss is ultimately a consequence of late gestational DBP exposure. Exposures to high doses of phthalate lead to decreased testis volume and cell number in utero [16], and DBP exposure leads to decreases in germ cell number in both the fetal and the postnatal testis, with exposures in early gestation leading directly to reduced germ cell number without induction of MNGs [6, 8, 42]. Although germ cell number in DBP-exposed rats has been reported to recover by PND 90 [6], some effects of phthalates on the seminiferous cords of fetal male rats persist into adulthood, including malformed seminiferous tubules and decreased spermatogenesis [17, 22, 59, 60]. Therefore, the degenerative effects of phthalates on fetal seminiferous cords may impact reproductive parameters in adults.

MNGs in the Context of Phthalate Toxicity

Environmental exposure of humans to phthalates in utero has led to concern for potential adverse effects on human male reproductive tract development [61, 62]. The male reproductive toxicity and risk assessment of in utero phthalate exposure has been understood primarily in the context of the antiandrogenic

action of phthalates in rats. The decrease in testosterone caused by phthalates has been presumed to be an upstream mechanistic event in phthalate toxicity in the fetal testis, as phthalates exert dose-additive antiandrogenic effects in this model [18, 19]. However, in addition to influencing steroidogenesis in the fetal Leydig cell, phthalates influence the development and differentiation of germ cells and seminiferous cords. Recent studies from our lab and others have indicated that the two sets of effects are not directly related. Treatment with antiandrogens such as the CYP17 inhibitor abiraterone and the androgen receptor antagonist flutamide led to reduced testosterone but failed to induce MNGs in human fetal testis xenografts [24] and rat fetal testis [3], respectively, while seminiferous cord effects of phthalate exposure occurred independent of antiandrogenic effects in mice [4, 7] and in human xenografts [23, 25]. Although the fetal testis of mice and humans is less sensitive than the rat to the antiandrogenic effects of phthalates [26–30], the seminiferous cord response is similar across species [8, 23]. Further, while it has long been presumed that the critical impacts of phthalate exposures stem from antiandrogenic effects during the masculinization programming window [9, 63], pathological effects on the seminiferous cord happen either early in gestation, including germ cell loss, or much later, including the generation of MNGs. These degenerative effects indicate that phthalate exposures outside of the masculinization programming window are relevant to human health. We have addressed the dose response for MNG induction in a previous rat study [16] and in xenotransplants from humans, rats, and mice [23]. In all three species, DBP induces MNGs strongly at doses of 100–250 mg/kg, with no effect observed at 50 mg/kg in rats. However, the limited dose-response data on MNGs and total germ cell number following in utero phthalate exposure represent an important data gap for understanding the mechanisms of phthalate toxicity and assessing their risk to human health.

ACKNOWLEDGMENT

The authors thank Melinda Golde for processing and cutting histological sections. We thank Drs. Natasha Catlin and Camelia Saffarini for assistance with scoring of histological sections. Conflict of interest statement: K. Boekelheide does occasional expert consulting with chemical and pharmaceutical companies. K. Boekelheide and S. Hall own stock in a small start-up biotechnology company (Semma Therapeutics) developing a wound healing therapeutic.

REFERENCES

1. Hannas BR, Lambright CS, Furr J, Howdeshell KL, Wilson VS, Gray LE, Jr. Dose-response assessment of fetal testosterone production and gene expression levels in rat testes following in utero exposure to diethylhexyl phthalate, diisobutyl phthalate, diisoheptyl phthalate, and diisononyl phthalate. Toxicol Sci 2011; 123:206–216.
2. Gray LE Jr, Ostby J, Furr J, Price M, Veeramachaneni DN, Parks L. Perinatal exposure to the phthalates DEHP, BBP, and DINP, but not DEP, DMP, or DOTP, alters sexual differentiation of the male rat. Toxicol Sci 2000; 58:350–365.
3. Mylchreest E, Sar M, Wallace DG, Foster PM. Fetal testosterone insufficiency and abnormal proliferation of Leydig cells and gonocytes in rats exposed to di(n-butyl) phthalate. Reprod Toxicol 2002; 16:19–28.
4. Gaido KW, Hensley JB, Liu D, Wallace DG, Borghoff S, Johnson KJ, Hall SJ, Boekelheide K. Fetal mouse phthalate exposure shows that Gonocyte multinucleation is not associated with decreased testicular testosterone. Toxicol Sci 2007; 97:491–503.
5. Parks LG, Ostby JS, Lambright CR, Abbott BD, Klinefelter GR, Barlow NJ, Gray LE Jr. The plasticizer diethylhexyl phthalate induces malformations by decreasing fetal testosterone synthesis during sexual differentiation in the male rat. Toxicol Sci 2000; 58:339–349.
6. Ferrara D, Hallmark N, Scott H, Brown R, McKinnell C, Mahood IK, Sharpe RM. Acute and long-term effects of in utero exposure of rats to di(n-butyl) phthalate on testicular germ cell development and proliferation. Endocrinology 2006; 147:5352–5362.
7. Lehraiki A, Racine C, Krust A, Habert R, Levacher C. Phthalates impair germ cell number in the mouse fetal testis by an androgen- and estrogen-independent mechanism. Toxicol Sci 2009; 111:372–382.
8. van den Driesche S, McKinnell C, Calarrao A, Kennedy L, Hutchison GR, Hrabalkova L, Jobling MS, Macpherson S, Anderson RA, Sharpe RM, Mitchell RT. Comparative effects of di(n-butyl) phthalate exposure on fetal germ cell development in the rat and in human fetal testis xenografts. Environ Health Perspect 2015; 123:223–230.
9. Foster PM. Disruption of reproductive development in male rat offspring following in utero exposure to phthalate esters. Int J Androl 2006; 29: 140–147; discussion 181–145.
10. Skakkebaek NE, Rajpert-De Meyts E, Main KM. Testicular dysgenesis syndrome: an increasingly common developmental disorder with environmental aspects. Hum Reprod 2001; 16:972–978.
11. Sharpe RM. Hormones and testis development and the possible adverse effects of environmental chemicals. Toxicol Lett 2001; 120:221–232.
12. Fisher JS. Environmental anti-androgens and male reproductive health: focus on phthalates and testicular dysgenesis syndrome. Reproduction 2004; 127:305–315.
13. McKinnell C, Mitchell RT, Walker M, Morris K, Kelnar CJ, Wallace WH, Sharpe RM. Effect of fetal or neonatal exposure to monobutyl phthalate (MBP) on testicular development and function in the marmoset. Hum Reprod 2009; 24:2244–2254.
14. Mitchell RT, Cowan G, Morris KD, Anderson RA, Fraser HM, McKenzie KJ, Wallace WH, Kelnar CJ, Saunders PT, Sharpe RM. Germ cell differentiation in the marmoset (*Callithrix jacchus*) during fetal and neonatal life closely parallels that in the human. Hum Reprod 2008; 23: 2755–2765.
15. Kleymenova E, Swanson C, Boekelheide K, Gaido KW. Exposure in utero to di(n-butyl) phthalate alters the vimentin cytoskeleton of fetal rat Sertoli cells and disrupts Sertoli cell-gonocyte contact. Biol Reprod 2005; 73: 482–490.
16. Boekelheide K, Kleymenova E, Liu K, Swanson C, Gaido KW. Dose-dependent effects on cell proliferation, seminiferous tubules, and male germ cells in the fetal rat testis following exposure to di(n-butyl) phthalate. Microsc Res Tech 2009; 72:629–638.
17. Barlow NJ, Foster PM. Pathogenesis of male reproductive tract lesions from gestation through adulthood following in utero exposure to di(n-butyl) phthalate. Toxicol Pathol 2003; 31:397–410.
18. Furr JR, Lambright CS, Wilson VS, Foster PM, Gray LE Jr. A short-term in vivo screen using fetal testosterone production, a key event in the phthalate adverse outcome pathway, to predict disruption of sexual differentiation. Toxicol Sci 2014; 140:403–424.
19. Howdeshell KL, Wilson VS, Furr J, Lambright CR, Rider CV, Blystone CR, Hotchkiss AK, Gray LE Jr. A mixture of five phthalate esters inhibits fetal testicular testosterone production in the Sprague-Dawley rat in a cumulative, dose-additive manner. Toxicol Sci 2008; 105:153–165.
20. Wilson VS, Lambright C, Furr J, Ostby J, Wood C, Held G, Gray LE Jr. Phthalate ester-induced gubernacular lesions are associated with reduced insl3 gene expression in the fetal rat testis. Toxicol Lett 2004; 146: 207–215.
21. Hannas BR, Lambright CS, Furr J, Evans N, Foster PM, Gray EL, Wilson VS. Genomic biomarkers of phthalate-induced male reproductive developmental toxicity: a targeted RT-PCR array approach for defining relative potency. Toxicol Sci 2012; 125:544–557.
22. Fisher JS, Macpherson S, Marchetti N, Sharpe RM. Human ''testicular dysgenesis syndrome'': a possible model using in-utero exposure of the rat to dibutyl phthalate. Hum Reprod 2003; 18:1383–1394.
23. Heger NE, Hall SJ, Sandrof MA, McDonnell EV, Hensley JB, McDowell EN, Martin KA, Gaido KW, Johnson KJ, Boekelheide K. Human fetal testis xenografts are resistant to phthalate-induced endocrine disruption. Environ Health Perspect 2012; 120:1137–1143.
24. Spade DJ, Hall SJ, Saffarini CM, Huse SM, McDonnell EV, Boekelheide K. Differential response to abiraterone acetate and di-n-butyl phthalate in an androgen-sensitive human fetal testis xenograft bioassay. Toxicol Sci 2014; 138:148–160.
25. Mitchell RT, Childs AJ, Anderson RA, van den Driesche S, Saunders PT, McKinnell C, Wallace WH, Kelnar CJ, Sharpe RM. Do phthalates affect steroidogenesis by the human fetal testis? Exposure of human fetal testis xenografts to di-n-butyl phthalate. J Clin Endocrinol Metab 2012; 97: E341–E348.
26. Habert R, Livera G, Rouiller-Fabre V. Man is not a big rat: concerns with traditional human risk assessment of phthalates based on their anti-androgenic effects observed in the rat foetus. Basic Clin Androl 2014; 24: 1–13.

27. Habert R, Muczynski V, Grisin T, Moison D, Messiaen S, Frydman R, Benachi A, Delbes G, Lambrot R, Lehraiki A, N'Tumba-Byn T, Guerquin MJ, et al. Concerns about the widespread use of rodent models for human risk assessments of endocrine disruptors. Reproduction 2014; 147: R119–R129.
28. Albert O, Jegou B. A critical assessment of the endocrine susceptibility of the human testis to phthalates from fetal life to adulthood. Hum Reprod Update 2014; 20:231–249.
29. Johnson KJ, Heger NE, Boekelheide K. Of mice and men (and rats): phthalate-induced fetal testis endocrine disruption is species-dependent. Toxicol Sci 2012; 129:235–248.
30. Johnson KJ, McDowell EN, Viereck MP, Xia JQ. Species-specific dibutyl phthalate fetal testis endocrine disruption correlates with inhibition of SREBP2-dependent gene expression pathways. Toxicol Sci 2011; 120: 460–474.
31. Saffarini CM, Heger NE, Yamasaki H, Liu T, Hall SJ, Boekelheide K. Induction and persistence of abnormal testicular germ cells following gestational exposure to di-(n-butyl) phthalate in p53-null mice. J Androl 2012; 33:505–513.
32. Conner MK, Boggs SS, Turner JH. Comparisons of in vivo BrdU labeling methods and spontaneous sister chromatid exchange frequencies in regenerating murine liver and bone marrow cells. Chromosoma 1978; 68:303–311.
33. Bak PM, Panos RJ. Protease antigen recovery decreases the specificity of bromodeoxyuridine detection in formalin-fixed tissue. J Histochem Cytochem 1997; 45:1165–1170.
34. Ridler TW, Calvard S. Picture thresholding using an iterative selection method. IEEE Trans Syst Man Cybern 1978; 8:630–632.
35. Boulogne B, Olaso R, Levacher C, Durand P, Habert R. Apoptosis and mitosis in gonocytes of the rat testis during foetal and neonatal development. Int J Androl 1999; 22:356–365.
36. Magaud JP, Sargent I, Clarke PJ, Ffrench M, Rimokh R, Mason DY. Double immunocytochemical labeling of cell and tissue samples with monoclonal anti-bromodeoxyuridine. J Histochem Cytochem 1989; 37: 1517–1527.
37. Allard EK, Hall SJ, Boekelheide K. Stem cell kinetics in rat testis after irreversible injury induced by 2,5-hexanedione. Biol Reprod 1995; 53: 186–192.
38. Lin H, Ge RS, Chen GR, Hu GX, Dong L, Lian QQ, Hardy DO, Sottas CM, Li XK, Hardy MP. Involvement of testicular growth factors in fetal Leydig cell aggregation after exposure to phthalate in utero. Proc Natl Acad Sci U S A 2008; 105:7218–7222.
39. Mahood IK, Hallmark N, McKinnell C, Walker M, Fisher JS, Sharpe RM. Abnormal Leydig cell aggregation in the fetal testis of rats exposed to di (n-butyl) phthalate and its possible role in testicular dysgenesis. Endocrinology 2005; 146:613–623.
40. Culty M. Gonocytes, the forgotten cells of the germ cell lineage. Birth Defects Res Part C Embryo Today 2009; 87:1–26.
41. Culty M. Gonocytes, from the fifties to the present: is there a reason to change the name? Biol Reprod 2013; 89:46.
42. Jobling MS, Hutchison GR, van den Driesche S, Sharpe RM. Effects of di(n-butyl) phthalate exposure on foetal rat germ-cell number and differentiation: identification of age-specific windows of vulnerability. Int J Androl 2011; 34:e386–e396.
43. Li Y, Cao Y, Wang F, Li C. Scrotal heat induced the Nrf2-driven antioxidant response during oxidative stress and apoptosis in the mouse testis. Acta Histochem 2014; 116:883–890.
44. Breslin WJ, Paulman A, Sun-Lin D, Goldstein KM, Derr A. The inhibin B (InhB) response to the testicular toxicants mono-2-ethylhexyl phthalate (MEHP), 1,3 dinitrobenzene (DNB), or carbendazim (CBZ) following short-term repeat dosing in the male rat. Birth Defects Res Part B Dev Reprod Toxicol 2013; 98:72–81.
45. Kudo S, Tanase H, Yamasaki M, Nakao M, Miyata Y, Tsuru K, Imai S. Collaborative work to evaluate toxicity on male reproductive organs by repeated dose studies in rats 23). A comparative 2- and 4-week repeated oral dose testicular toxicity study of boric acid in rats. J Toxicol Sci 2000; 25(spec no):223–232.
46. Hansen DA, Esakky P, Drury A, Lamb L, Moley KH. The aryl hydrocarbon receptor is important for proper seminiferous tubule architecture and sperm development in mice. Biol Reprod 2014; 90:8.
47. Fujiwara Y, Ogonuki N, Inoue K, Ogura A, Handel MA, Noguchi J, Kunieda T. t-SNARE Syntaxin2 (STX2) is implicated in intracellular transport of sulfoglycolipids during meiotic prophase in mouse spermatogenesis. Biol Reprod 2013; 88:141.
48. Cortes D, Thorup J, Visfeldt J. Multinucleated spermatogonia in cryptorchid boys: a possible association with an increased risk of testicular malignancy later in life? APMIS 2003; 111:25–30; discussion 31.
49. Greenbaum MP, Iwamori N, Agno JE, Matzuk MM. Mouse TEX14 is required for embryonic germ cell intercellular bridges but not female fertility. Biol Reprod 2009; 80:449–457.
50. Greenbaum MP, Ma L, Matzuk MM. Conversion of midbodies into germ cell intercellular bridges. Dev Biol 2007; 305:389–396.
51. Greenbaum MP, Yan W, Wu MH, Lin YN, Agno JE, Sharma M, Braun RE, Rajkovic A, Matzuk MM. TEX14 is essential for intercellular bridges and fertility in male mice. Proc Natl Acad Sci U S A 2006; 103: 4982–4987.
52. Russell LD, Vogl AW, Weber JE. Actin localization in male germ cell intercellular bridges in the rat and ground squirrel and disruption of bridges by cytochalasin D. Am J Anat 1987; 180:25–40.
53. Rabionet M, Bayerle A, Jennemann R, Heid H, Fuchser J, Marsching C, Porubsky S, Bolenz C, Guillou F, Grone HJ, Gorgas K, Sandhoff R. Male meiotic cytokinesis requires ceramide synthase 3-dependent sphingolipids with unique membrane anchors. Hum Mol Genet 2015; 24:4792–4808.
54. Gondos B, Hobel CJ. Ultrastructure of germ cell development in the human fetal testis. Z Zellforsch Mikrosk Anat 1971; 119:1–20.
55. Fukuda T, Hedinger C, Groscurth P. Ultrastructure of developing germ cells in the fetal human testis. Cell Tissue Res 1975; 161:55–70.
56. Franchi LL, Mandl AM. The ultrastructure of germ cells in foetal and neonatal male rats. J Embryol Exp Morphol 1964; 12:289–308.
57. Huckins C, Clermont Y. Evolution of gonocytes in the rat testis during late embryonic and early post-natal life. Arch Anat Histol Embryol 1968; 51: 341–354.
58. Picut CA, Remick AK, de Rijk EP, Simons ML, Stump DG, Parker GA. Postnatal development of the testis in the rat: morphologic study and correlation of morphology to neuroendocrine parameters. Toxicol Pathol 2015; 43:326–342.
59. Mahood IK, Scott HM, Brown R, Hallmark N, Walker M, Sharpe RM. In utero exposure to di(n-butyl) phthalate and testicular dysgenesis: comparison of fetal and adult end points and their dose sensitivity. Environ Health Perspect 2007; 115(suppl 1):55–61.
60. Dostal LA, Chapin RE, Stefanski SA, Harris MW, Schwetz BA. Testicular toxicity and reduced Sertoli cell numbers in neonatal rats by di(2-ethylhexyl)phthalate and the recovery of fertility as adults. Toxicol Appl Pharmacol 1988; 95:104–121.
61. Swan SH, Main KM, Liu F, Stewart SL, Kruse RL, Calafat AM, Mao CS, Redmon JB, Ternand CL, Sullivan S, Teague JL. Decrease in anogenital distance among male infants with prenatal phthalate exposure. Environ Health Perspect 2005; 113:1056–1061.
62. Huang PC, Kuo PL, Chou YY, Lin SJ, Lee CC. Association between prenatal exposure to phthalates and the health of newborns. Environ Int 2009; 35:14–20.
63. Scott HM, Mason JI, Sharpe RM. Steroidogenesis in the fetal testis and its susceptibility to disruption by exogenous compounds. Endocr Rev 2009; 30:883–925.